Radiation of spin waves from magnetic vortex cores by their dynamic motion and annihilation processes

Ki-Suk Lee, SangKook Choi, and Sang-Koog Kim

Citation: Applied Physics Letters **87**, 192502 (2005); doi: 10.1063/1.2128478
View online: http://dx.doi.org/10.1063/1.2128478
View Table of Contents: http://scitation.aip.org/content/aip/journal/apl/87/19?ver=pdfcov
Published by the AIP Publishing

Radiation of spin waves from magnetic vortex cores by their dynamic motion and annihilation processes

Ki-Suk Lee, SangKook Choi, and Sang-Koog Kim[a)]
Nanospintronics Laboratory, School of Materials Science and Engineering, College of Engineering, Seoul National University, Seoul 151-744, Korea

(Received 4 February 2005; accepted 1 September 2005; published online 1 November 2005)

We report on micromagnetic simulation results of radiation of strong spin waves from the cores of magnetic vortices driven by their dynamics motion or the annihilation of a vortex-antivortex pair in a rectangular shaped magnetic thin film. Such strong spin-waves are distinguished from spin wave modes typically excited in patterned magnetic elements. The spin wave excitation with relatively low frequencies of 0–22 GHz are associated with the shape of an element, a magnetization configuration, and an applied magnetic field, while dominating spin waves in the higher frequencies of 22–96 GHz are driven by either the motion or annihilation of vortex cores present in the confined element. The latter case yields much higher amplitudes than the former does. It is found that large torques applied at the local area of the vortex cores, driven by the large exchange fields in the core region during their dynamic motion and collapse, induce a rapid energy dissipation into the surrounding areas through the spin-wave excitation and subsequent propagation. In addition, it is found that the strong spin waves radiated by the dynamic evolution processes of the vortex cores propagate well into a long stripe-shaped magnetic wire. Such traveling spin waves can be applicable for a new generation of magnetic logic devices. © *2005 American Institute of Physics*.
[DOI: 10.1063/1.2128478]

Spin-wave excitations in confined magnetic thin films begin to attract much attention because of its practical applications to magnetic logic devices[1] as well as its fundamental interest.[2–4] Both theoretical and experimental studies have thus been increased in numbers for the exploration of the spatial and temporal characteristics of spin waves excited in micrometer-scale magnetic elements.[5–17] It is known that the characteristic properties of spin waves are determined by the intrinsic material parameters of exchange and dipole interactions and an external magnetic field as well as the size and shape of a system.[5–9] Fundamentally, it has been of great interest how the frequencies and spatial configurations of their eigenmodes are governed by these parameters. From a technological point of view, a logical operation using spin waves is also of a great interest because they can deliver information with the controllable phases of spin waves being propagating in magnetic media, which is applicable for a new generation of logic devices. For example, Hertel *et al.*[1] demonstrated using micromagnetic simulations that the phase of a spin wave can be controllable with magnetic domain walls formed in a waveguide medium. For making the spin waves practical in its applications, it is required that spin waves should be radiated strongly and then propagate well inside a spin waveguide. In this letter, we report on micromagnetic simulation results of strong radiations of spin waves through the dynamic motion or annihilation of the cores of magnetic vortices present in a rectangular shaped magnetic thin film, triggered by an external magnetic field.

In order to carry out the micromagnetic simulations[18] of spin-wave radiations, we utilized a rectangular shaped element of an Fe film which includes 5 vortices and 2 antivortices at an equilibrium state of the spatial distribution of local magnetization vectors (**M**) without a magnetic field $\mathbf{H}_a$, as shown in Fig. 1. The characteristic features of the existing vortices are represented by the **M** orientation of their cores and the in-plane **M** orientation of circular or cross Bloch lines, as shown in Fig. 1(b).[19] In the micromagnetic modeling, we used a constant cell size of $5\times5\times20$ nm^3, an exchange constant $A=2.1\times10^{-11}$ (J/m), a saturation magnetization $M_s=1.7\times10^6$ (A/m), an anisotropy constant $K=0$, and a damping parameter $\alpha=0.01$.

A temporal evolution of the equilibrium spatial variation of the local **M** shown in Fig. 1 is found to approach toward a new equilibrium state under a static magnetic field of $H_a=100$ Oe that is applied along the short axis of the rectangular element. As already reported in our earlier work,[19,20] not only vortices but also antivortices play crucial roles in the **M**

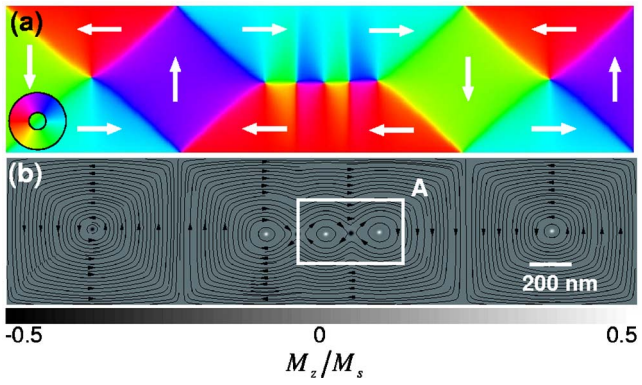

FIG. 1. (Color online) A spatial distribution of local **M** at equilibrium in a rectangular shaped model system of an Fe film with a lateral dimension of 3.0×0.7 μm^2 and a 20 nm thickness. Colors in (a) represent the in-plane orientations of the local **M**, as noted by the colored wheel, while the gray-colored scale in (b) indicates the out-of-plane components of the local **M** normalized by its saturation magnetization, M_z/M_s. The streamlines with small arrows shown in (b) are displayed to show the characteristic features of individual vortices and antivortices present in the rectangular shaped element.

[a)]Author to whom correspondence should be addressed; electronic mail: sangkoog@snu.ac.kr

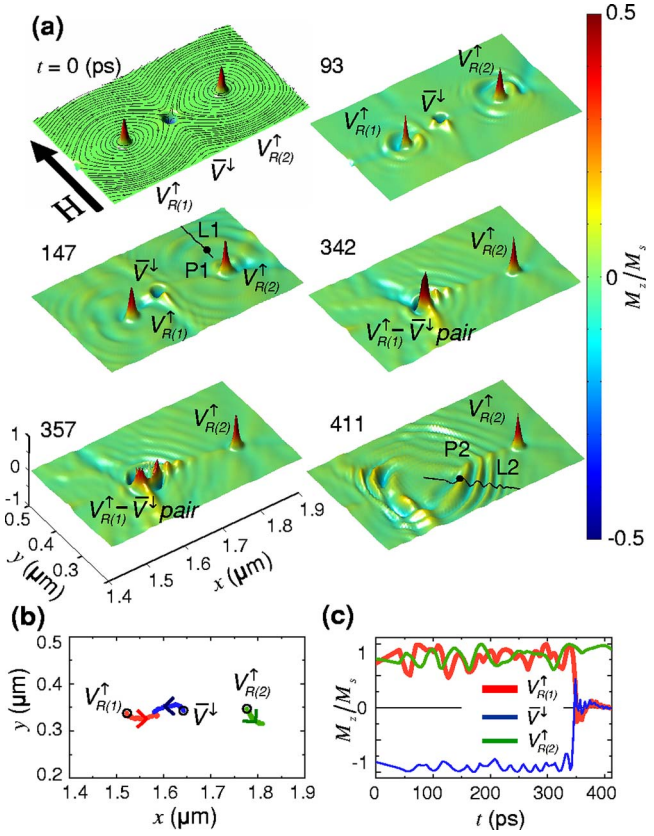

FIG. 2. (Color online) Images of the temporal evolution of the spatial configuration of local **M** in the area indicated by "A" in Fig. 1(b) under a static magnetic field of H_a=100 Oe applied along the direction noted by the black arrow. The colors indicate the magnitudes of local M_z/M_s. (b) and (c) show the temporal variations of the positions and the M_z/M_s values, respectively, for the cores of the three different vortices.

dynamics through their propagation and annihilation due to their attractive interactions. Figure 2(a) shows snapshot images of the temporal evolution taken at given times t, as noted. For t=93 ps, the spin waves radiated around each vortex core driven by their dynamic motions further spread into their surrounding areas. Much stronger spin waves with large amplitudes start to be radiated at t=342 ps, when the vortex $V^{\uparrow}_{R(1)}$ and the antivortex $\bar{V}^{\downarrow}$ meet, and then collapse. For the movie file of the dynamic evolution, see Ref. 21. The positions of the individual cores of $V^{\uparrow}_{R(1)}$, $V^{\uparrow}_{R(2)}$, and $\bar{V}^{\downarrow}$ and their values of M_z/M_s versus t are also shown in Figs. 2(b) and 2(c), respectively.

For a better understanding of the existing modes of the radiated spin waves, the variations of M_z/M_s with distance l at t=147 and 411 ps along the lines denoted as "L1" and "L2" in Fig. 2(a) are plotted together with their Fourier transformed (FT) spectra, as shown in Fig. 3(a). As seen in the M_z/M_s versus l, the spin waves radiated during the annihilation process of a vortex-antivortex pair have much larger amplitudes than those driven by the motion of the vortex cores. From their FT spectra, we can see a large contrast in the amplitudes of the spin waves radiated by two different ways of the motion of vortex cores and the annihilation of a vortex-antivortex pair. Much higher FT power at lower wave numbers k (near zero k) for the "L1" line seems to be associated with spin-wave excitations typically formed by an external magnetic field and an inhomogeneous internal magnetic field that varies with the shape of a micrometer-size

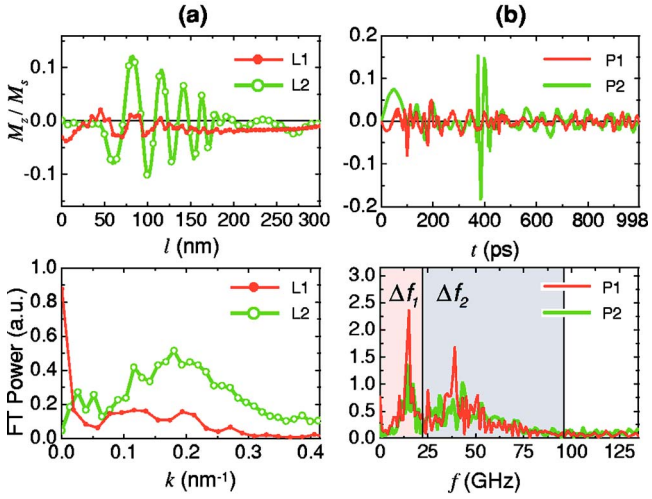

FIG. 3. (Color online) (a) Variations of M_z/M_s with distance along the lines indicated by "L1" and "L2" in Fig. 2(a), and their Fourier-transformed spectra. (b) Temporal evolutions of M_z/M_s in a range of t=0 ~ 998 ps at the two different positions indicated by "P1" and "P2" in Fig. 2(a), and their Fourier transformed f spectra.

element as well as the local **M** configuration.[9–12]

In Fig. 3(b), the M_z/M_s versus t at two different positions indicated by "P1" (near $V^{\uparrow}_{R(2)}$ core) and "P2" (near $V^{\uparrow}_{R(1)}-\bar{V}^{\downarrow}$ pair) shown in Fig. 2(a) are compared together with their frequency f spectra obtained from their FTs. From these spectra, it is clearly found that the excited spin waves have a wide range of frequencies, where each frequency is associated with individual characteristic modes excited by different causes as well as radiated from many other neighboring vortices. From a direct comparison of the frequency spectra obtained at the two different positions, we find that there is no distinct difference in the general profile of the f spectra of the wave modes at the "P1" and "P2" positions, while the magnitudes of their FT powers are somewhat different. From such complicated frequency spectra, we cannot classify all the spin wave modes, but their dominating modes in the two different frequency regions of Δf_1=0–22 GHz and Δf_2=22–96 GHz can be differentiated by making the inverse FTs of the individual frequency spectra for each cell in the corresponding frequency ranges. Figure 4 shows the

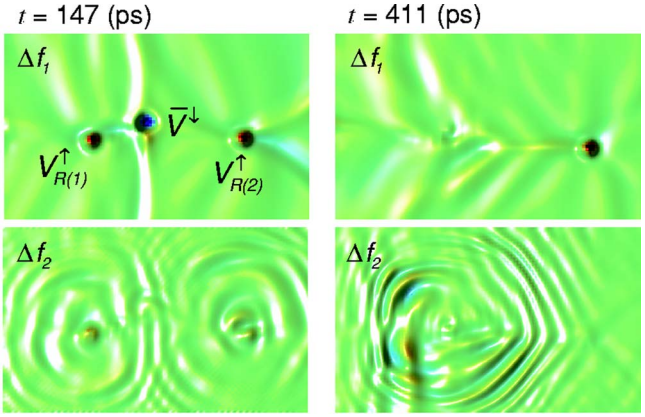

FIG. 4. (Color online) Plane-view images of the spatial configurations of the two different dominating modes at t=147 and 411 ps, which are obtained from the inverse FTs of the frequency spectra of individual cells in the two different ranges of $0 \leq f < 22$ GHz, and $22 \leq f \leq 96$ GHz, as displayed by the shaded regions in Fig. 3(b).

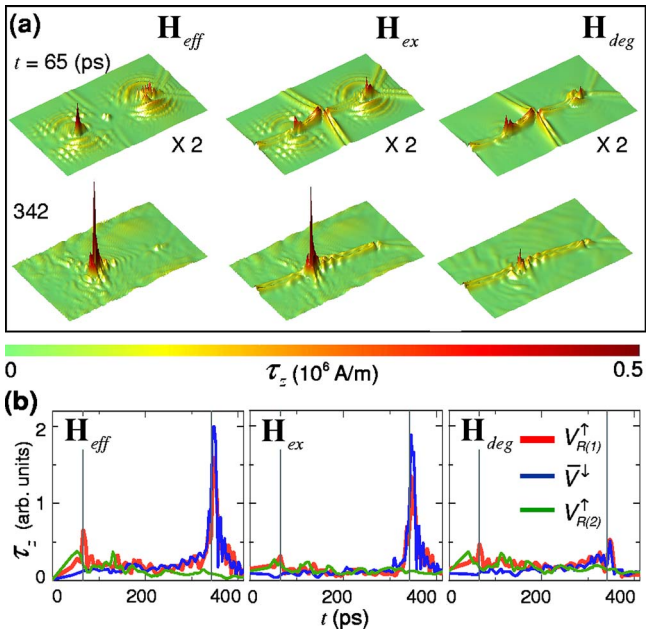

FIG. 5. (Color online) (a) shows the perspective-view images of the perpendicular component of torques, $\tau_z=(\mathbf{m}\times\mathbf{H})\cdot\hat{\mathbf{e}}_z$, exerting on the individual cells in the same area as that seen in Fig. 2, for $t=65$ and 342 ps. Each column in (a) shows $\mathbf{H}_{\text{eff}}$, $\mathbf{H}_{\text{ex}}$, and $\mathbf{H}_{\text{deg}}$ contributions to the total torque. (b) shows the temporal variations of the average torques within 3×3 cells around the cores of the three different vortices shown in Fig. 2. The vertical lines indicate $t=65$ and 342 ps.

snapshot images taken at $t=147$ and 411 ps for the two different types of spin wave modes separated by their inverse FTs in the Δf_1 and Δf_2 ranges. Their movie files are also provided.[21] It is certain that the spin wave modes in the range of 22 GHz$\leqslant f\leqslant$96 GHz are associated primarily with radiations from vortex cores during their motions ($t=147$ ps) and their annihilation process ($t=411$ ps). The dominating modes in the low frequency range ($f<22$ GHz) are not associated with the dynamic evolution process of the vortex cores, but associated with the inhomogeneous internal field in the rectangular element as well as the external magnetic field.

Next, to clarify the main cause of the strong radiations of spin waves, we calculate the temporal evolution of total torques $\boldsymbol{\tau}_{\text{eff}}=\mathbf{m}\times\mathbf{H}_{\text{eff}}$ exerting on the unit magnetization vector $\mathbf{m}$ of individual cells, and the individual contributions of the exchange field $\mathbf{H}_{\text{ex}}$, the demagnetization (or magnetostatic) field $\mathbf{H}_{\text{deg}}$, and the Zeeman field $\mathbf{H}_a$ to the $\boldsymbol{\tau}_{\text{eff}}$. Figure 5 shows the perpendicular component of the torques τ_z for the individual contributions of $\mathbf{H}_{\text{eff}}$, $\mathbf{H}_{\text{ex}}$, and $\mathbf{H}_{\text{deg}}$. The Zeeman field contribution is not presented here because of its negligible contribution compared to the others. The sizable spin waves being propagating in the vicinity of the cores of $V^{\uparrow}_{R(1)}$ and $V^{\uparrow}_{R(2)}$ at $t=147$ and 411 ps are certainly due to the large τ_z strongly localized to their cores, developed at earlier times (see Fig. 5), compared to the negligible τ_z in their surrounding areas. In particular, strong spin waves with much large amplitudes present after $t=342$ ps are driven by the extremely large τ_z formed at the local area where the cores of $V^{\uparrow}_{R(1)}$ and $\bar{V}^{\uparrow}$ encounter, as shown in Fig. 5. The large torques exerting on such a pin-point area are rapidly released through the excitations and propagations of the strong spin waves, which is a means of the rapid release of highly concentrated energy from the vortex cores into their surrounding areas. The magnitudes of τ_z contributed individually from $\mathbf{H}_{\text{eff}}$, $\mathbf{H}_{\text{ex}}$, and $\mathbf{H}_{\text{deg}}$ at the localized areas of the cores of the three different vortices are plotted versus t in Fig. 5(b). It is also proven that the largest torque at $t=342$ ps initiates an excitation of spin waves and that the major contribution to the torque is $\mathbf{H}_{\text{ex}}$. Since the Zeeman field contribution to the total torque is negligible compared to the others, the large torques exerting on the vortex cores result primarily from changes in the positions of vortex cores and in the magnitudes of their M_z/M_s values. Such spin wave modes with large amplitudes can be distinguished from spin wave modes typically excited from several other ways in micrometer-scale elements, such as by tilting and rotating $\mathbf{M}$ orientations,[1,8,17] as well as by applying an $\mathbf{H}_a$.

With these findings mentioned above, we also investigated an injection of spin waves strongly radiated from a well-known vortex state in a disk shaped magnetic element into a long-stripe magnetic-film waveguide. The injected spin waves in the waveguide were well propagated with the characteristic frequencies and wave numbers of their dominating modes that are allowed in the magnetic waveguide. More details and further studies of the wave propagations, not shown here, will be reported elsewhere. Strong spin waves being propagating well in the magnetic nanowires may be promising for their applications to a logical operation in a new generation of logic devices.

This work was supported by the KOSEF through the q-Psi at Hanyang University.

[1]R. Hertel, W. Wulfhekel, and J. Kirschner, Phys. Rev. Lett. **93**, 257202 (2004).
[2]L. R. Walker, Phys. Rev. **105**, 390 (1957).
[3]B. A. Kalinikos and A. N. Slavin, J. Phys. C **19**, 7013 (1986).
[4]S. O. Demokritov, B. Hillebrands, and A. N. Slavin, Phys. Rep. **348**, 441 (2001).
[5]C. Mathieu, J. Jorzick, A. Frank, S. O. Demokritov, A. N. Slavin, B. Hillebrands, B. Bartenlian, C. Chappert, D. Decanini, F. Rousseaux, and E. Cambril, Phys. Rev. Lett. **81**, 3968 (1998).
[6]R. Zivieri and F. Nizzoli, Phys. Rev. B **71**, 014411 (2005).
[7]B. A. Ivanov and C. E. Zaspel, Phys. Rev. Lett. **94**, 027205 (2005).
[8]V. Novosad, M. Grimsditch, K. Yu. Guslienko, P. Vavassori, Y. Otani, and S. D. Bader, Phys. Rev. B **66**, 052407 (2002).
[9]K. Yu. Guslienko, S. O. Demokritov, B. Hillebrands, and A. N. Slavin, Phys. Rev. B **66**, 132402 (2002).
[10]K. Yu. Guslienko, R. W. Chantrell, and A. N. Slavin, Phys. Rev. B **68**, 024422 (2003).
[11]J. Jorzick, S. O. Demokritov, B. Hillebrands, M. Bailleul, C. Fermon, K. Y. Guslienko, A. N. Slavin, D. V. Berkov, and N. L. Gorn, Phys. Rev. Lett. **88**, 047204 (2002).
[12]C. Bayer, J. P. Park, H. Wang, M. Yan, C. E. Campbell, and P. A. Crowell, Phys. Rev. B **69**, 134401 (2004).
[13]J. P. Park, P. Eames, D. M. Engebretson, J. Berezovsky, and P. A. Crowell, Phys. Rev. Lett. **89**, 277201 (2002).
[14]T. M. Crawford, M. Covington, and G. J. Parker, Phys. Rev. B **67**, 024411 (2003).
[15]M. Belov, Z. Liu, R. D. Sydora, and M. R. Freeman, Phys. Rev. B **69**, 094414 (2004).
[16]M. Buess, R. Hollinger, T. Haug, K. Perzlmaier, U. Krey, D. Pescia, M. R. Scheinfein, D. Weiss, and C. H. Back, Phys. Rev. Lett. **93**, 077207 (2004).
[17]M. Grimsditch, G. K. Leaf, H. G. Kaper, D. A. Karpeev, and R. E. Camley, Phys. Rev. B **69**, 174428 (2004).
[18]We used the OOMMF code. See http://math/nist.gov/oommf.
[19]K.-S. Lee, B.-W. Kang, Y.-S. Yu, and S.-K. Kim, Appl. Phys. Lett. **85**, 1568 (2004).
[20]S.-K. Kim, K.-S. Lee, B.-W. Kang, K.-J. Lee, and J. B. Kortright, Appl. Phys. Lett. **86**, 052504 (2005).
[21]See EPAPS Document No. E-APPLAB-87-002545 for three movie files (.avi). This document may be retrieved via the EPAPS homepage (http://www.aip.org/pubservs/epaps.html) or from ftp.aip.org in the directory /epaps/. See the EPAPS homepage for more information.